(3) W. P. Jencks, "Catalysis in Chemistry and Enzymology", Part III, McGraw-Hill, New York, 1969.
(4) M. L. Bender, "Mechanisms of Homogeneous Catalysis from Protons to Proteins", Wiley, New York, 1971, p 108 ff.
(5) R. D. Gandour and R. L. Schowen, Eds., "Transition States of Biochemical Processes", Plenum Press, New York, 1978.
(6) C. J. Collins and N. S. Bowman, Eds., "Isotope Effects in Chemical Reactions", Van Nostrand-Reinhold, Princeton, N.J., 1970.
(7) W. W. Cleland, M. H. O'Leary, and D. B. Northrop, "Isotope Effects on Enzyme-Catalyzed Reactions", University Park Press, Baltimore, Md., 1977.
(8) M. Wolfsberg and M. J. Stern, *Pure Appl. Chem.*, **8**, 225 (1964); M. J. Stern and M. Wolfsberg, *J. Pharm. Sci.*, **54**, 849 (1965); R. E. Weston, Jr., *Science*, **158**, 332 (1967); W. A. Van Hook in ref 5, Chapter 1.
(9) W. E. Buddenbaum and V. J. Shiner, Jr., in ref 7.
(10) J. L. Hogg in ref 5; V. J. Shiner, Jr., in ref 6; J. L. Kirsch in ref 7, and references cited by these authors.
(11) (a) M. L. Bender and M. S. Feng, *J. Am. Chem. Soc.*, **82**, 6318 (1960); J. M. Jones and M. L. Bender, *ibid.*, **82**, 6322 (1960); (b) cf. E. A. Halevi and Z. Margolin, *Proc. Chem. Soc., London*, 174 (1964).
(12) C. G. Mitton and R. L. Schowen, *Tetrahedron Lett.*, 5803 (1968).
(13) A. Fry in ref 6.
(14) J. H. Schachtschneider and R. G. Snyder, *Spectrochim. Acta*, **19**, 117 (1963).
(15) E. B. Wilson, J. C. Decius, and P. C. Cross, "Molecular Vibrations", McGraw-Hill, New York, 1955.
(16) For example, G. W. Burton, L. B. Sims, J. C. Wilson, and A. Fry, *J. Am. Chem. Soc.*, **99**, 3371 (1977); G. W. Burton, L. B. Sims, and D. J. McLennan, *J. Chem. Soc., Perkin Trans. 2*, 1847 (1977).
(17) W. D. Gwinn, *J. Chem. Phys.*, **55**, 477 (1971).
(18) (a) L. Pauling, "The Nature of the Chemical Bond", 3rd ed., Cornell University Press, Ithaca, N.Y., 1960, p 239. For the use of the Pauling bond order in transition-state structural questions, see (b) H. S. Johnston, "Gas Phase Reaction Rate Theory", Ronald Press, New York, 1966; (c) H. B. Bürgi, J. D. Dunitz, and E. Shefter, *J. Am. Chem. Soc.*, **95**, 5065 (1973); *Acta Crystallogr., Sect. B*, **30**, 1517 (1975); P. Murray-Rust, H. B. Bürgi, and J. D. Dunitz, *ibid.*, **97**, 921 (1975); E. Shefter in ref 5; (d) G. M. Maggiora and R. L. Schowen in "Bioorganic Chemistry", Vol. 1, E. E. van Tamelen, Ed., Academic Press, New York, 1977, pp 173–229.
(19) R. D. Gandour, G. M. Maggiora, and R. L. Schowen, *J. Am. Chem. Soc.*, **96**, 6967 (1974).
(20) R. W. Kilb, C. C. Lin, and E. B. Wilson, *J. Chem. Phys.*, **26**, 1695 (1957).
(21) R. Janoschek, H. Preuss, and G. Diercksen, *Int. J. Quantum Chem.*, **1**, 649 (1967).
(22) A. Timidei and G. Zerbi, *Z. Naturforsch. A*, **25**, 1729 (1970).
(23) P. Cossee and J. H. Schachtschneider, *J. Chem. Phys.*, **44**, 97 (1965).
(24) A. Serralach, R. Mayer, and H. H. Gunthard, *J. Mol. Spectrosc.*, **52**, 94 (1974).
(25) K. Fukushima and B. Zwolinski, *J. Mol. Spectrosc.*, **26**, 368 (1968).
(26) H. M. R. Arbouiv-van der Veen and J. C. Leyte, *J. Cryst. Mol. Struct.*, **2**, 17 (1972).
(27) G. A. Crowder and D. Jackson, *Spectrochim. Acta, Part A*, **27**, 2505 (1971).
(28) H. B. Bürgi, J. D. Dunitz, J. M. Lehn, and G. Wipff, *Tetrahedron*, **30**, 1563 (1974).
(29) P. A. Hogan, R. D. Gandour, G. M. Maggiora, and R. L. Schowen, unpublished calculations.
(30) There is an extensive literature on techniques of generating critical coordinates in model calculations (see the review by W. A. Van Hook in ref 5, p 36 ff, the recent work of Yankwich and his school, such as G. J. Wei and P. E. Yankwich, *J. Chem. Phys.*, **62**, 2200 (1975), and earlier papers, and the discussions of Buddenbaum and Shiner.[9]) The choice made here is reasonable on chemical grounds, since the formation of the C^2–O^8 bond and the partial rupture of the C^2–O^1 bond (thus an asymmetric motion of O^8–C^2–O^1) comprise the most important elements of the chemical process.
(31) F. H. Westheimer, *Chem. Rev.*, **61**, 265 (1961).
(32) C. A. Lewis, Jr., and R. Wolfenden, *Biochemistry*, **16**, 4886 (1977), and references cited therein.
(33) J. J. Ortiz and E. H. Cordes, *J. Am. Chem. Soc.*, **100**, 7080 (1978).
(34) E. A. Hill and S. A. Milosevich, *Tetrahedron Lett.*, 4553 (1976).
(35) Z. Bilkadi, R. de Lorimier, and J. F. Kirsch, *J. Am. Chem. Soc.*, **97**, 3417 (1975).
(36) V. Okano, L. do Amaral, and E. H. Cordes, *J. Am. Chem. Soc.*, **98**, 4201 (1976).
(37) L. do Amaral, M. P. Bastos, H. G. Bull, and E. H. Cordes, *J. Am. Chem. Soc.*, **95**, 7369 (1973).
(38) L. do Amaral, M. P. Bastos, H. G. Bull, J. J. Ortiz, and E. H. Cordes, *J. Am. Chem. Soc.*, **101**, 169 (1979).
(39) P. R. Young and P. E. McMahon, paper in preparation; P. R. Young, R. C. Bogseth, and E. G. Reitz, paper in preparation.
(40) I. M. Kovach, J. L. Hogg, J. Rodgers, T. Raben, K. Halbert, and R. L. Schowen, *J. Am. Chem. Soc.*, in press.
(41) E. R. Thornton, *Annu. Rev. Phys. Chem.*, **17**, 349 (1966).

Theoretical Search for a New Nonclassical Carbonium Ion: The σ-Allyl Cation[1,2]

Kenny B. Lipkowitz,*[3a] Raima M. Larter,[3b] and Donald B. Boyd*[3c]

Contribution from the Department of Chemistry, Indiana-Purdue University at Indianapolis, Indianapolis, Indiana 46205, the Department of Chemistry, Indiana University, Bloomington, Indiana 47401, and Lilly Research Laboratories, Eli Lilly and Company, Indianapolis, Indiana 46206. *Received March 12, 1979*

Abstract: In order to assess the desirability of synthesizing a polycyclic carbonium ion which might exhibit pure pp–σ bonding between the electron-deficient centers, molecular orbital calculations are done on a model system composed of three stacked methyl groups $(CH_3)_3^+$ with collinear carbons. Applied are six MO methods spanning a spectrum of complexity, ranging from semiempirical extended Hückel, CNDO/2, and MINDO/3 to ab initio with STO-3G, double-ζ, and 6-31G* basis sets. Whereas CNDO/2, MINDO/3, and STO-3G predict the most stable structure to be symmetrical with a planar central CH_3 unit and pyramidal terminal CH_3 units, the two more lengthy methods predict an asymmetric $CH_3CH_3\cdots CH_3$ geometry to be preferred. As shown by electron-density maps of the symmetric structure, the σ counterparts of the three familiar π allylic orbitals are present. All MO methods agree that the central carbon of both the symmetric and asymmetric geometries bears more electron density than the terminal carbons and that the peripheral atoms bear most of the cationic charge. MINDO/3 calculations show $[C(CH_3)_3]_3^+$ to be unsuitable as a model. Also, MINDO/3 indicates that $C_3H_9^+$ isomers with nonlinear backbones are more stable than the $(CH_3)_3^+$ model.

A generally accepted definition of the term "nonclassical ion" has been presented by Brown and Schleyer.[4,5] "A nonclassical carbonium ion is a positively charged species which cannot be represented adequately by a single Lewis structure. Such a cation contains one or more carbon or hydrogen bridges joining the two electron-deficient centers. The bridging atoms have coordination numbers higher than usual, typically five or more for carbon and two or more for hydrogen. Such ions contain two-electron, three- (or multiple-) center bonds including a carbon or hydrogen bridge."

In order to analyze the nature of bonding in carbonium ions, it will be convenient to focus attention initially on the 2p atomic orbitals. The type of interaction arising from a particular arrangement of p orbitals has been the focal point of several recent studies.[6,7] A pp–π overlap (A) is, of course, a symmetric combination of parallel p orbitals which are perpendicular to

0002-7863/80/1502-0085$01.00/0

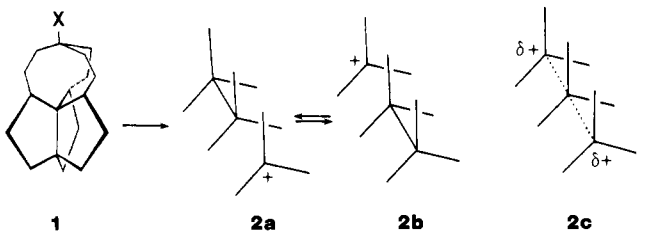

Figure 1. Ionization of an appropriately capped propellane may result in an equilibrating ion **2a**, **2b**, or a delocalized structure **2c**. Methylene bridges are omitted from the drawings of **2** for clarity.

a bond axis, and there is a single nodal plane through the bond axis. The combination of collinear p orbitals that are cylindrically symmetric about the bond axis is called pp-σ overlap (C). These forms represent the extrema of a broad spectrum of canted p orbitals where a decrease in the level of pp-π character occurs with concomitant increase in pp-σ character as the p orbitals are canted toward each other (B).[8]

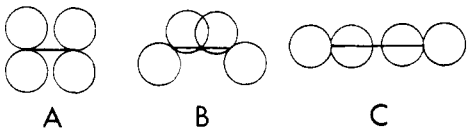

One complication in the explanation of nonclassical carbonium ion behavior centers around the fact that three-center, two-electron bonding involves both pp-π and pp-σ contributions. Indeed, no system has been designed specifically to factor out one type of overlap leaving the other to be cleanly studied. In this paper, we introduce a novel system that substantially eliminates pp-π interactions between the electron-deficient centers and maximizes pp-σ interactions.

To wit, the solvolysis of a polycyclic system like **1** could give rise to a novel carbonium ion **2** (Figure 1). Space-filling molecular models suggest that **1** is sterically crowded and, in fact, would tend to lose X^- so that the incipient cationic carbon can be displaced along the propellane axis toward the central carbon. Dreiding models also indicate that nonbonded contacts between some of the hydrogens of **1** are very short. Similarly, inchoate **2** is very crowded when the electron-deficient carbon is sp^2 hybridized. But when this carbon moves still closer to the central carbon, such as when the former is sp^3 hybridized with a vacant orbital pointing *toward* the central carbon, then some of the strain is relieved. Thus, it is possible that a molecule like **1** would even experience a driving force to expel X^- and juxtapose the axial carbons so that the positive charge can be delocalized through the core of the molecule. Two of the possibilities that can be envisioned for **2** (Figure 1) are (1) interconverting classical structures **2a** $\rightleftarrows$ **2b**, or (2) a nonclassical structure **2c** where charge is more evenly spread over the axial centers. The latter situation, in essence, is a pp-σ allyl cation that may be expected to behave differently than a typical pp-π allyl cation.

It may be argued that the initially formed ion is a tertiary carbocation and that, in general, tertiary carbonium ions are sufficiently stable to not exhibit σ bridging.[4] Thus the 2-methyl-2-norbornyl cation (R = CH_3) is unquestionably classical, whereas it is possible that the secondary analogue (R = H) is bridged. There exist, however, a few extreme cases

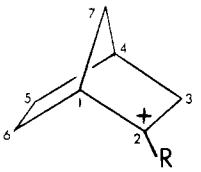

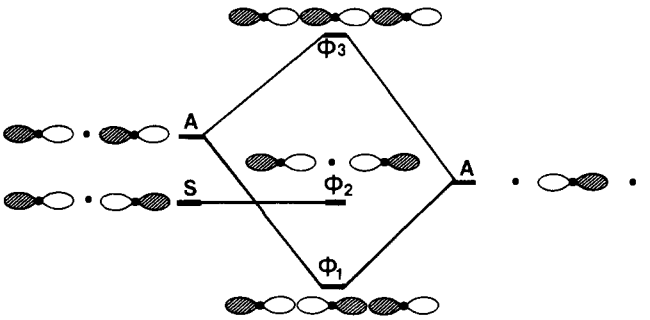

Figure 2. Qualitative molecular orbital mixing diagram for the three collinear p orbitals overlapping in σ fashion. Orbitals are classified according to whether they are symmetric (S) or antisymmetric (A) with respect to reflection through a plane of symmetry intersecting the central carbon atom perpendicular to the C···C···C axis.

where tertiary cations will bridge. For instance, direct participation from the double bond and cyclopropyl moiety has been demonstrated for the 7-methyl-7-norbornenyl and Coates' cations, respectively.[7,9] Certainly the high polarizability of the participating bonds in these examples compared to the rather nonpolarizable C_6-C_1 σ bond in the 2-methyl-2-norbornyl cation is, at least in part, responsible for the observed differences in bridging. It is well established that the polarizability of an alkyl carbon-carbon σ bond is highest *along the bond axis*.[10] The ratio of longitudinal to transverse polarizabilities of the C-C bond is almost 4:1. Based on this, the 2-methyl-2-norbornyl cation with its angular relationship between the cationic center C_2 and the C_6-C_1 is less appropriate for σ bridging than is **2**, which has a collinear relationship between the initial cationic center and the propellane bond. Also, the impulse to argue on the basis of extrapolating information about σ bridging from well-characterized systems (e.g., norbornyl) to our novel system **2** may not be justified because very little is known about pure pp-σ bonding in carbonium ions.

Besides its unique bonding and steric features, **2** is also of interest because it contains a carbon in a trigonal bipyramidal[11a] arrangement. It is the purpose of this paper to shed some light on the electronic structure of **2** using quantum-mechanical techniques.

A qualitative picture of the σ allyl system can be obtained by considering first the in-phase and out-of-phase combinations of the p_σ atomic orbitals on the terminal carbons. The in-phase combination has A-type symmetry. These combinations are expected to be nearly degenerate because of the small overlap between the two terminal carbons.[11b] The mixing of these fragment orbitals with the central carbon's p atomic orbital, which by necessity has A-type symmetry, results in a lifting of this near degeneracy as shown in Figure 2. The two fragment orbitals of A symmetry interact strongly to form bonding and antibonding combinations. In effect, ϕ_1, ϕ_2, and ϕ_3 are the σ counterparts of the familiar[12,13] π allylic orbitals.

Calculations and Results

The picture in Figure 2 can be made quantitative using ab initio and all-valence-electron semiempirical molecular orbital methods. Because we will be treating a system not investigated before, it is wise to use a selection of different methods which span a spectrum[14] of accuracy. Then the predictions of the different methods can be compared and artifacts of the approximations or basis set can more likely be spotted. The semiempirical methods that we employ are the familiar EH,[15] CNDO/2,[16] and MINDO/3[17] procedures. Ab initio (restricted Hartree-Fock) MO calculations[18] were done with STO-3G,[19] double-ζ,[20] and STO-6-31G*[21] basis sets. A priori one would suppose that the accuracy of these methods increases roughly in the order listed.

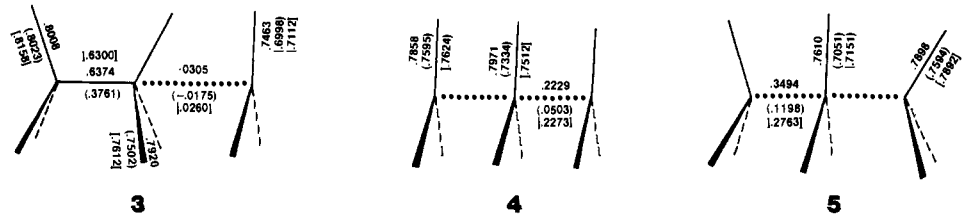

Figure 3. Mulliken overlap populations of ions **3**, **4**, and **5**. Values are obtained from wave functions expanded over STO-3G, double-ζ (parentheses), and 6-31G* (brackets) basis sets.

Because of the large size of **2** ($C_{18}H_{27}^+$), ab initio calculations would be impractical even with something like the Dacre–Elder formalism.[22] Also at the semiempirical level, **2** would be quite expensive to treat in a geometry optimization scheme. Hence it is imperative to use a model of **2**. One such model is $(CH_3)_3^+$. It consists of a stack of three methylium ions to which two extra electrons are added to bring the total to 20 valence electrons (and 6 core electrons). A Dreiding model of **2** suggests that the three radial C–C bonds to each of the three axial carbons are *roughly eclipsed*. Hence we will do most of our calculations on $(CH_3)_3^+$ with the carbons collinear and the hydrogens eclipsed. Use of an eclipsed geometry will, if anything, overestimate repulsions and hence offset any overestimation of the attractive forces that some of the MO methods[2] may be prone to give.

Also, we will examine a *staggered* geometry for $(CH_3)_3^+$ (see Figure 5 for the results of staggering the central methyl) and some alternate $C_3H_9^+$ isomers with other three-center bonding. At first glance, a model more suitable than $(CH_3)_3^+$ might be the tri-*tert*-butyl cation $[C(CH_3)_3]_3^+$. Whereas this system preserves the tertiary nature of the carbonium ion, the methyl groups introduce additional steric repulsions not present in **2**. Some calculations were done on $[C(CH_3)_3]_3^+$ as outlined below, but the repulsions between the hydrogens so overpowered all the other effects that this model proved less helpful than $(CH_3)_3^+$.

The $(CH_3)_3^+$ Model. Three geometries for the eclipsed form of $(CH_3)_3^+$ can be considered. Of these, **3** involves a methylium ion interacting with ethane, whereas **4** and **5** are symmetric

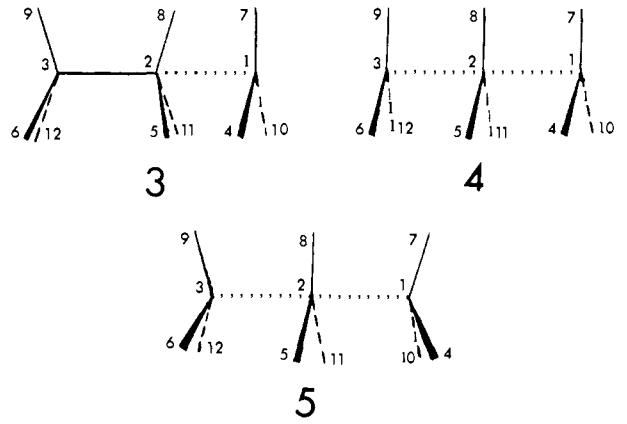

with $C_1C_3 = C_2C_3$, so that the cationic charge is more delocalized. For the ab initio and initial CNDO/2 calculations, the following bond lengths and angles were used. Ions **4** and **5** are identical except that the terminal methyls in **5** are pyramidal rather than planar. In **5** the C_2–C_1–H bond angles were held fixed at 109.5°. In both **4** and **5** the C–H bond lengths were assumed to be constant at 1.079 Å,[23] and the energy was minimized by moving C_1 and C_3 (with attendant H's) toward the central methyl. In **3**, eclipsed ethane was built using a C–C bond length of 1.54 Å, C–H bond lengths of 1.079 Å, and C–C–H bond angles in the ethane moiety of 109.5°. The energy was minimized by adjusting only the distance between the planar methyl and ethane groups. Final geometries, total energies, and net charges for **3**, **4**, and **5** calculated with the three ab initio methods and the CNDO/2 semiempirical method are presented in Table I. Overlap populations from the ab initio wave functions are shown in Figure 3.

In further calculations, fully optimized geometries for $(CH_3)_3^+$ were obtained using MINDO/3 and CNDO/2.[24] For these runs, the only constraints were to enforce the collinearity of the carbons and the eclipsing of the hydrogens. The final MINDO/3 geometry of **5** served as input for EH calculations. The results of these MINDO/3, CNDO/2, and EH calculations are summarized in Table II. The symmetric geometry (**5**) represents an energy minimum on the energy hypersurface.

The minimum basis set results, as well as the semiempirical results, indicate that **5** is most stable, **3** is second most stable, and **4** is least stable. Structure **5** has the end carbons more nearly sp^3 hybridized, and, as noted before, molecular models show that a geometry like that of **5** could be accommodated into the rigid framework of **2**. The ab initio energy differences between **4** and **5** can be associated with the increased overlap population between the carbons of **5** (Figure 3).

Whereas STO-3G predicted **3** to be 6 kcal/mol *less* stable than **5**, the larger basis set procedures (double ζ and 6-31G*) both predict **3** to be 11–13 kcal/mol *more* stable than **5**. Thus, with the more flexible basis sets the classical model **3** is more stable than either of the nonclassical models **4** or **5**. We will comment further on the contrast between the predictions of the elaborate and other methods later in the paper.

The geometries calculated by the ab initio and the semiempirical methods are of interest. As expected, the C_1C_2 bond lengths decrease in going from **3** to **4** to **5**. This is a direct consequence of diminution of nonbonded steric repulsion between the hydrogens; both ab initio and semiempirical methods display this trend (Table I). Both CNDO/2 (Tables I and II) and MINDO/3 (Table II) tend to underestimate the C_1C_2 bond lengths for all ions studied when compared to the ab initio results (Table I). CNDO/2 is known to give unreliable results when investigating certain pp–σ nonbonded interactions[1] and to underestimate nonbonded repulsions in general.[2]

At the outset of this paper we anticipated a mixing of orbitals that would lower one of the A combinations below the S combination of p orbitals (Figure 2). Once again, all of the calculations qualitatively confirm this ordering of molecular orbitals. As expected, the quantitative aspects of the energies of these levels differ from one computational scheme to the next. From the ab initio calculation (STO-3G) the highest occupied molecular orbital (HOMO) transforms as A_2'' in the D_{3h} point group. This corresponds to the orbital labeled ϕ_1 in Figure 2. The lowest unoccupied molecular orbital (LUMO) corresponds to ϕ_2 and transforms as A_1', while the next to lowest unoccupied molecular orbital (NLUMO) corresponds to ϕ_3 and has A_2'' symmetry. At 3-Å separation between the outer and central carbons as well as at the energy minima, both **4** and **5** keep ϕ_1, ϕ_2, and ϕ_3 as the HOMO, LUMO, and NLUMO, respectively. That is to say, there are no orbital crossings in the range 1.8–3.0 Å.

The MINDO/3 results are somewhat different. At the en-

Table I. Calculational Results for $(CH_3)_3^+$ Models

		3	4	5
		STO-3G		
minimized geometry		C_1C_2 = 2.50 Å	$C_1C_2 = C_2C_3$ = 2.00 Å	$C_1C_2 = C_2C_3$ = 1.80 Å
total energy, au		−116.944 39	−116.912 43	−116.954 23
net charges	C_1	−0.1246	−0.3158	−0.3562
	C_2	−0.5394	−0.6313	−0.6735
	C_3	−0.4781	−0.3158	−0.3562
	H_4	+0.3386	+0.2655	+0.2568
	H_5	+0.1727	+0.2233	+0.2779
	H_6	+0.2027	+0.2655	+0.2568
		Double ζ		
minimized geometry		C_1C_2 = 2.70 Å	$C_1C_2 = C_2C_3$ = 2.05 Å	$C_1C_2 = C_2C_3$ = 1.80 Å
total energy, au		−118.423 07	−118.372 99	−118.405 72
net charges	C_1	−0.0408	−0.2508	−0.3474
	C_2	−0.5828	−0.8784	−0.7877
	C_3	−0.5040	−0.2508	−0.3474
	H_4	+0.3192	+0.2671	+0.2652
	H_5	+0.1881	+0.2593	+0.2972
	H_6	+0.2019	+0.2671	+0.2652
		STO6-31G*		
minimized geometry		C_1C_2 = 2.70 Å	$C_1C_2 = C_2C_3$ = 2.05 Å	$C_1C_2 = C_2C_3$ = 1.75 Å
total energy, au		−118.440 82	−118.386 01	−118.420 26
net charges	C_1	−0.0148	−0.1925	−0.1953
	C_2	−0.5652	−0.8664	−0.9028
	C_3	−0.3306	−0.1925	−0.1953
	H_4	+0.3180	+0.2573	+0.2374
	H_5	+0.1474	+0.2359	+0.2895
	H_6	+0.1715	+0.2573	+0.2374
		CNDO/2		
minimized geometry		C_1C_2 = 1.70 Å	$C_1C_2 = C_2C_3$ = 1.60 Å	$C_1C_2 = C_2C_3$ = 1.50 Å
total energy, au		−27.7583	−27.7209	−27.8795
net charges	C_1	+0.1240	+0.0381	+0.0643
	C_2	−0.0178	−0.0283	−0.0217
	C_3	+0.0245	+0.0381	+0.0643
	H_4	+0.1012	+0.0862	+0.0639
	H_5	+0.1137	+0.1322	+0.1695
	H_6	+0.0656	+0.0862	+0.0639

Table II. Fully Optimized Geometries of $(CH_3)_3^+$ from MINDO/3 and CNDO/2 (in Parentheses) Calculations

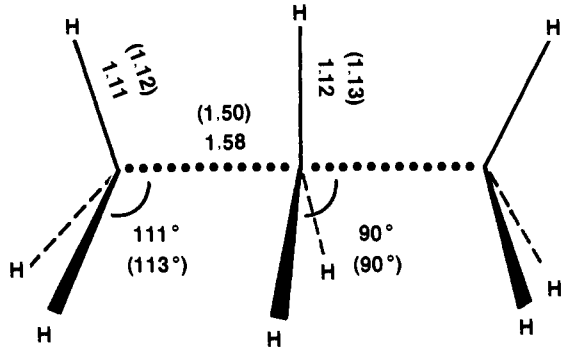

MINDO/3[a] net charges	C_1	+0.1755	(−0.0115)	EH net charges	C_1	+0.1206
	C_2	−0.0716	(−0.2813)		C_2	+0.0286
	H_4	+0.0439	(+0.1104)		H_4	+0.0458
	H_5	+0.1525	(+0.2139)		H_5	+0.1521

[a] MINDO/3D net charges are given in parentheses. These values follow from a Mulliken population analysis of the $S^{-1/2}$ deorthogonalized MINDO/3 eigenvectors.

ergy minimum for ion **5**, ϕ_1 character occurs in the next to the next highest occupied molecular orbital (NNHOMO), ϕ_2 is still the LUMO, and ϕ_3 character is most clearly associated with the highest unoccupied molecular orbital (HUMO). CNDO/2 results are somewhat similar to MINDO/3, and show that ϕ_1 occurs as the NHOMO, ϕ_2 as the LUMO, and

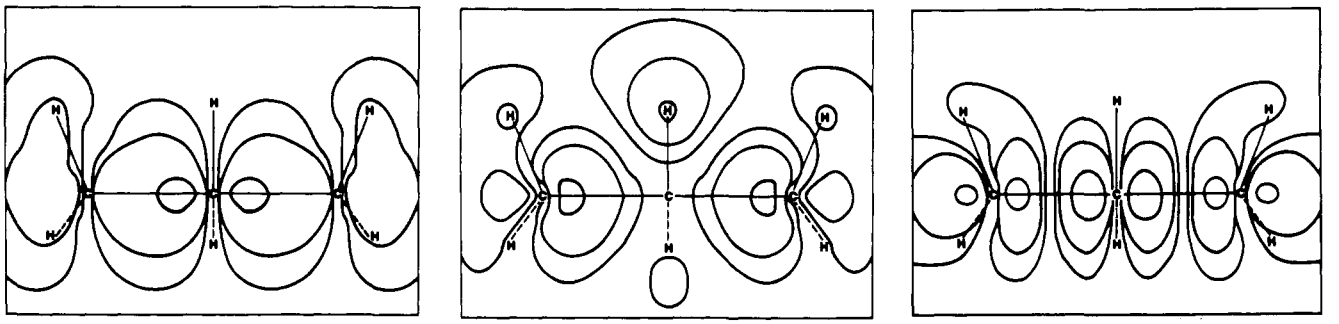

Figure 4. Electron density maps of the MINDO/3D MOs of symmetrical $(CH_3)_3^+$. The three panels show the next to the next highest occupied MO (left), the lowest unoccupied MO (middle), and the highest unoccupied MO (right). Each map covers 5.2 × 3.9 Å and shows the density calculated in the plane through H_9-C_3-C_2-C_1-H_7. Interatomic axes in this plane are shown in solid lines; projections of other bond axes onto this plane are denoted by dashed lines. Since density, rather than the MO itself, is plotted, the phases of the orbital lobes are not shown. The phases of ϕ_1, ϕ_2, and ϕ_3 are depicted in Figure 2. An occupation number of two electrons is assumed for the sake of computing the density contours of the nominally unoccupied MOs. Starting at the edges of the panels, the contours are at 0.001, 0.01, and 0.1 e bohr^{-3}.

ϕ_3 as the HUMO. Correlation diagrams for the variation of the CNDO/2 eigenvalues as a function of C···C distance in **4** and **5** show that the A_2'' HOMO at 2.50 Å drops below a degenerate pair of orbitals that transform as E′ at short C···C separation. In both cases the LUMO uneventfully increases in energy as C···C is reduced to the minimum energy distance. The EH method places ϕ_1 as the NNHOMO, ϕ_2 as the LUMO, and ϕ_3 as the NNNLUMO (i.e., the fourth lowest unoccupied MO) of **5**.

Electron-density maps[25] of the three σ allylic type orbitals are shown in Figure 4. These particular maps were computed from the deorthogonalized MINDO/3 eigenvectors for the MINDO/3 optimized geometry of $(CH_3)_3^+$. The analogous EH MOs are practically identical in shape. Because the MINDO/3 orbitals are computed in the neglect-of-overlap (NDO) approximation, they were deorthogonalized by an $S^{-1/2}$ transformation.[26] The ϕ_1 orbital in Figure 4 (MINDO/3's NNHOMO) is, of course, the only one of the three allylic orbitals to be occupied in the ground state. The ϕ_1 orbital has σ bonding character between each pair of carbons. The ϕ_2 orbital (MINDO/3's LUMO) has nonbonding character with lobes on the two terminal carbons. The LUMO has some C–H σ* character, but the NLUMO (A_1') has more; the $C_2$2s LCAO coefficient is especially large in the NLUMO. The ϕ_3 orbital (MINDO/3's HUMO) is antibonding between both carbon pairs as indicated by the nodal surfaces which dissect the density between the carbons. Our electron-density maps of ϕ_1, ϕ_2, and ϕ_3 may be compared to the π_1, π_2*, and π_3* orbitals, respectively, as plotted for the allyl cation by Jorgensen and Salem.[12] The analogy between the two sets is apparent.

Consider next the charge distributions of **3**–**5**. We preface this section with the comment that the Mulliken population analysis and the various MO schemes can have difficulties in giving conceptually consistent charges.[27] Ideally, one would like to see the various computational techniques give similar answers, but, as experience has proven, eigenvectors (which ultimately give rise to bond overlap populations and net atomic charges) depend on the MO method used. Furthermore, within one computational scheme the calculated charge densities will vary depending on the type of population analysis used. The quantitative diversity of charges in Tables I and II is thus not too surprising.

Mulliken population analysis of the ab initio wave functions indicates considerable net negative charge on the carbons, whereas the positive charge is dispersed over the hydrogens for **3**, **4**, and **5**. CNDO/2 suggests that only the middle carbon will carry a negative charge. MINDO/3 net charges agree with those from CNDO/2 in that **5** will have the central carbon negatively charged. In contrast, EH indicates that all atoms will bear a positive charge. A discussion of which is the correct charge density becomes somewhat polemic, and we shall avoid this argument entirely. We can, however, predict that the central methyl of nonclassical species **4** and **5** will differ from the terminal methyls. All the MO methods bear out this prediction with the central carbon shouldering more electron density than the terminal ones.

From a spectroscopist's point of view, the charges in our models of **2** are most interesting, for, as Dewar has already pointed out,[28] the norbornyl cation is a very poor model with which to argue the classical–nonclassical problem. The calculated charges of the nonclassical π complex, **6**, and the time-averaged classical species, **7a** and **7b**, are similar enough

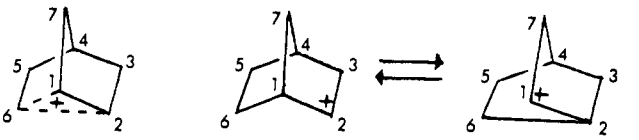

6 **7a** **7b**

to obfuscate the issue. The MINDO/3 net atomic charges of these ions reported by Dewar[28] are presented in Table III to illustrate this point. In contrast, the charges of a rapidly equilibrating form of **3** compared to the charges of **4** or **5** lend themselves to differentiating the structures. Using the net charges from Tables I and II for the classical ion **3**, averages were calculated as ½(**3a** + **3b**) (where **3a** and **3b** are two interconverting classical ions). These data are presented in Table III also. The average values should be compared to the corresponding net atomic charges for ions **4** and **5** presented in Table I. The difference in net charge on the *outer* carbons in **3** vs. **4** or **5** is not very large and could lead to the same problem of distinguishing the classical and nonclassical structures as in the norbornyl case. But, on the other hand, the difference in net charge on the *central* carbon of **3** vs. **4** or **5** is quite large, at least for the ab initio values. Hence the charge on the central atom of σ-allyl cations could in principle serve as a good handle with which to study classical–nonclassical behavior using techniques such as ESCA and NMR.

Other Models. Earlier, some other possible model structures of **2** were mentioned. MINDO/3 calculations were done on **8**, $[C(CH_3)_3]_3^+$, which can be viewed as a methylated form of the $(CH_3)_3^+$ model. The enlarged model, while requiring considerable computer time, was of interest because it was thought that it would more closely represent the tertiary centers of the carbonium ion **2**.

Four forms of **8** are considered. All have the tertiary carbons collinear. The first form, **8a**, consists of a substituted eclipsed ethane interacting with a $C(CH_3)_3^+$ species. The second form, **8c**, is the same as **8a**, except that the ethane is staggered. The

Table III. Comparison of the Net Atomic Charges for Nonclassical Structures with the Mean of Those for the Classical Structures

	2-Norbornyl Cations						
	C_1	C_2	C_3	C_4	C_5	C_6	C_7
6a[a]	+0.142	+0.142	+0.015	+0.035	+0.023	+0.057	+0.015
$\frac{1}{2}$(**7a** + **7b**)[a]	+0.181	+0.181	−0.003	+0.040	+0.018	+0.090	−0.003
	σ-Allyl Cations						
	C_1	C_2	C_3	H_4	H_5	H_6	
$\frac{1}{2}$(**3a** + **3b**)[b]	+0.074	−0.018	+0.074	+0.083	+0.114	+0.083	
$\frac{1}{2}$(**3a** + **3b**)[c]	−0.301	−0.539	−0.301	+0.271	+0.173	+0.271	
$\frac{1}{2}$(**3a** + **3b**)[d]	−0.272	−0.583	−0.272	+0.261	+0.188	+0.261	
$\frac{1}{2}$(**3a** + **3b**)[e]	−0.173	−0.565	−0.173	+0.245	+0.147	+0.245	

[a] MINDO/3 values. [b] CNDO/2 values. [c] STO-3G values. [d] Double-ζ GTO values. [e] 6-31G* values.

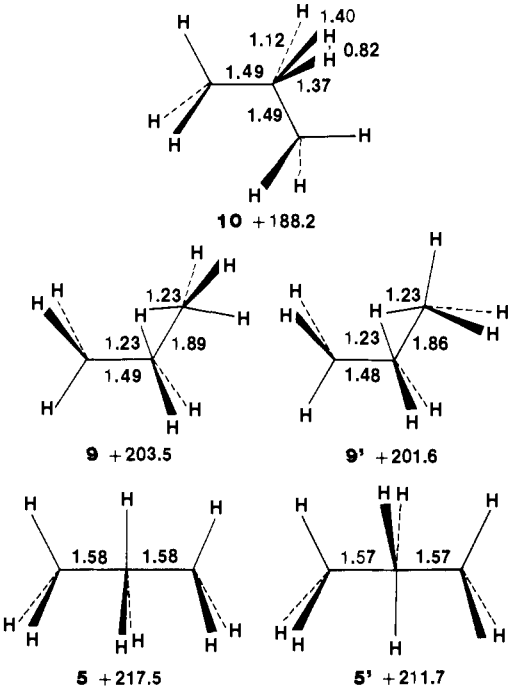

Figure 5. MINDO/3 heats of formation (kcal/mol) and optimized molecular geometries (bond lengths in Å) for some $C_3H_9^+$ isomers. Other bond lengths and angles from the energy minimization process are not shown for sake of clarity.

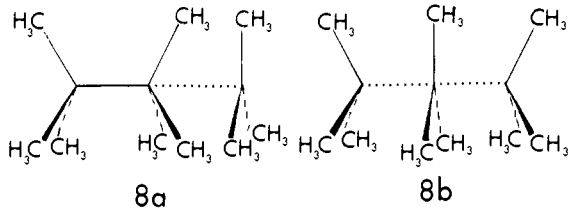

third form, **8b,** starts with the central $C(CH_3)_3$ equally separated and eclipsed with respect to the terminal groups. **8d** differs from **8b** by having the central $C(CH_3)_3$ staggered. Bond lengths and angles were allowed to optimize, except for C–H (1.11 Å) and C–C–H (111°), which were selected at near-optimum MINDO/3 values.

Structure **8c** is most stable by MINDO/3. The final C–C distances are 1.64 and 6.10 Å. Thus, the model exists as a substituted ethane which weakly interacts with a $C(CH_3)_3^+$ cation. The separation between the two parts is great enough so that the C_{tert}–C_{tert}–CH_3 bond angles are 112° at both ends of the ethane. The positive charge is almost totally on the separated $C(CH_3)_3^+$ moiety, which is planar as expected for a classical tertiary carbonium ion. About 5 kcal/mol less stable is **8a,** which has bond lengths and angles essentially the same as in **8c**. Structures **8b** and **8d** are least stable. The calculations could not be made to reach a minimum for these because, in effect, it consisted of three $C(CH_3)_3$ moieties drifting about 4 Å apart on an apparently very flat potential energy surface.

It must be concluded that $[C(CH_3)_3]_3^+$ serves as a poor model of **2** because the steric repulsions between the methyl groups swamp out the C···C···C interactions. The H···H repulsions prevent the initial carbonium ion $C(CH_3)_3^+$ from approaching very closely to the substituted ethane. However, such H···H repulsions would not exist in the caged system **2**.

Finally, we consider some other $C_3H_9^+$ models for comparison. Various isomers of $C_3H_9^+$ (but not **3**–**5**) have been studied previously both experimentally[29] and theoretically.[30] In general, these studies have shown that isomers **9** and **10** with

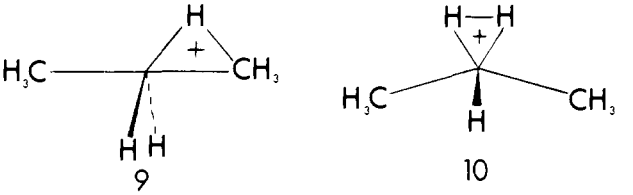

three-center bonding are relatively stable. Our own calculations on these and the $(CH_3)_3^+$ model are summarized in Figure 5. The MINDO/3 method was used to completely optimize the geometry of each of the conformations shown. Staggering of the methyls in **9** (vs. **9'**) and in **5'** (vs. **5**) results in a lowering of ΔH_f (increase in stability) of about 2 and 6 kcal/mol, respectively. Also, the C···C bond lengths shorten as expected.

In these calculations (Figure 5) all geometrical variables were free to equilibrate according to the MINDO/3 framework. Thus, the fact that the collinear $(CH_3)_3^+$ model **5** remained collinear indicates that this structure exists at a minimum on the energy hypersurface. Likewise, the other structures shown also represent either local or global minima. A symmetrical $C_3H_9^+$ isomer **11** was also studied, but it opened

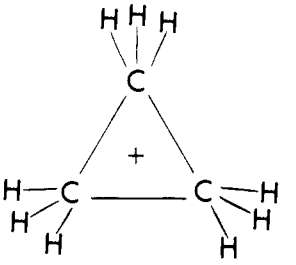

up to **10** during the geometry optimization process.

As can be seen in Figure 5, **10** is most stable. The conformers of **9** are of intermediate energy, and the collinear models (**5** and

5') are relatively less stable. In contrast, earlier ab initio 4-31G calculations predicted **9** and **10** to be of similar stability (but much more stable than **11**).[30] The latest experimental evidence[29] points toward **10** having a lower energy than **9,** which is consistent with our MINDO/3 predictions. The qualitative energy differences predicted by MINDO/3 seem reasonably satisfactory, although quantitatively the energies in Figure 5 may not have much significance. It appears that the protonated propane isomers involving three-center bonding between hydrogens and carbons are preferred over those with three-center bonding between only carbons. The collinear $C_3H_9^+$ structure **5** must be regarded as too unstable to be of importance as an entity in itself, but it may still be appropriate for use as a model for a larger caged system (**2**).

Concluding Remarks

Several ab initio and semiempirical MO procedures have been applied to $(CH_3)_3^+$. This is the simplest and most practical model of a hypothetical polycyclic carbocation **2** with unique pp-σ interactions between the electron-deficient carbons. Whereas the semiempirical and STO-3G MO methods indicate that delocalization (**2c,** Figure 1) can exist, the larger basis set results favor the existence of a classical structure such as **2a,** which could be in equilibrium with an equivalent structure **2b,** provided that the interconversion barrier, whatever it is, is not too high.

A definitive conclusion on the nature of a cation formed from **1** is not possible. One precluding factor is that there is some uncertainty in extrapolating results from primary to a tertiary carbonium ion system. Thus, the large surface area for dispersal[31] of ionic charge would lower the electron demand of the electron-deficient center and could favor the classical forms. On the other hand, the strain present in **2** and the unique pp-σ bonding (which our calculations have purposely underestimated owing to the eclipsing in **3**–**5**) may allow a nonclassical structure to exist. Still another possibility is that **2,** whatever its electronic structure, would be a transient species in the solvolysis of **1** and subsequent rearrangements would occur.

Another factor preventing a definitive conclusion is that none of the quantum-mechanical methods used here explicitly incorporates electron correlation.[32] In a study of $C_3H_7^+$ carbocations,[33] predictions from 6-31G* were shown to be upset when correlated wave functions were obtained and, in fact, the cruder MINDO/3 results agreed with the correlated ones. It has been suggested[28] that conventional semiempirical treatments, such as CNDO, are too inaccurate to treat carbocations, and that a very large basis set, such as 6-31G*, is needed in the ab initio calculations. The $C_3H_7^+$ study[33] indicates that not even 6-31G* may be adequate to compare classical and nonclassical structures. Our experience with $(CH_3)_3^+$ does, indeed, indicate a difference in relative energies between CNDO and 6-31G*. But also the MINDO/3 method gives the same predictions as CNDO/2 for the stability of **5** vs. **3**. At this point it is not possible to pick one of the procedures used in this paper as clearly more reliable than another for predicting the structure of $(CH_3)_3^+$. The contrast in the relative energies of the more elaborate ab initio methods and the other MO methods illustrates the hazard of basing conclusions on only a single method. As is well known, all the methods used in our study are frequently used to study carbocations.[28,30,33,34]

The possibility remains open that **1,** if made, could be converted to the novel system **2c** with its unique pp-σ bonding. If **2c** can exist, we expect the σ-allylic MOs to be like those described herein.

Acknowledgment. The Indiana University Research Foundation and the Indiana University Computer Network generously provided use of their equipment. We thank A. Szabo for helpful discussions and advice on the use of some of the computer programs and H. H. Jaffé for his enthusiastic interest and help. This work was supported in part by a grant from the Research Corporation.

References and Notes

(1) Part 3 of the series "$p_\sigma p_\sigma$ Interactions in Organic Molecules". For parts 1 and 2, see K. B. Lipkowitz and R. M. Larter, *Tetrahedron Lett.,* 33 (1978); K. B. Lipkowitz, *J. Am. Chem. Soc.,* **100,** 7535 (1978).
(2) Part 15 of the series "Mapping Electron Density in Molecules". For part 14, see D. B. Boyd, *J. Phys. Chem.,* **82,** 1407 (1978).
(3) (a) Indiana-Purdue University; (b) Indiana University; (c) Lilly Research Laboratories.
(4) H. C. Brown, "The Nonclassical Ion Problem", Plenum Press, New York, 1977, Chapter 4.
(5) See also H. C. Brown, *Tetrahedron,* **32,** 179 (1976); G. A. Olah, *Acc. Chem. Res.,* **9,** 41 (1976).
(6) L. A. Paquette, T. G. Wallis, T. Kempe, G. G. Christoph, J. P. Springer, and J. Clardy, *J. Am. Chem. Soc.,* **99,** 6946 (1977); G. G. Christoph, J. L. Muthard, L. A. Paquette, M. C. Bohm, and R. Gleiter, *ibid.,* **100,** 7782 (1978); K. Yano, M. Isobe, and K. Yoshida, *ibid.,* **100,** 6166 (1978); K. B. Lipkowitz, unpublished work.
(7) L. A. Paquette, *Angew. Chem., Int. Ed. Engl.,* **17,** 106 (1978).
(8) Fastidious use of the terms pp-σ and pp-π would require us to point out that there can be *both* σ and π overlap between the 2p atomic orbitals on any two centers regardless of their spatial relationship in a molecule. It is always possible to choose a local coordinate syster for a pair of atoms with the σ orbitals collinear with the internuclear axis and π orbitals orthogonal to the axis; see, e.g., D. B. Boyd and W. N. Lipscomb, *J. Chem. Phys.,* **48,** 4955 (1968), and references cited therein. The term "pp-σ interaction" discussed in ref 1 is used somewhat more loosely to refer to the situation where a 2p orbital which nominally (and mainly) is involved in a π-electron system also overlaps in σ fashion with a 2p orbital on another atom which can be involved in a second π-electron system. In the present paper, "pp-σ interaction" pertains to the situation where a 2p orbital (or some hybrid of p and s orbitals) overlaps in σ fashion with a similar orbital on another center to such an extent that a mutual perturbation of the orbitals takes place.
(9) See Chapter 14 of ref 4.
(10) For a review of molecular reactivity and polarizability, see R. J. W. LeFèvre, *Adv. Phys. Org. Chem.,* **3,** 49 (1965).
(11) (a) E. D. Jemmis, J. Chandrasekhar, and P. v. R. Schleyer, *J. Am. Chem. Soc.,* **101,** 527 (1979); T. R. Forbus, Jr., and J. C. Martin, *ibid.,* **101,** 5057 (1979). (b) For other examples of near degeneracy created by mixing weakly interacting orbitals, see the discussion of interaction diagrams for laticyclic topologies by M. J. Goldstein and R. Hoffmann, *J. Am. Chem. Soc.,* **93,** 6193 (1971).
(12) W. L. Jorgensen and L. Salem, "Organic Chemist's Book of Orbitals", Academic Press, New York, 1973, p 137.
(13) For MO calculations on the usual π allyl system, see, e.g., R. Hoffmann, *J. Chem. Phys.,* **40,** 2480 (1964); S. D. Peyerimhoff and R. F. Buenker, *ibid.,* **51,** 2528 (1969); D. T. Clark and D. R. Armstrong, *Theor. Chim. Acta,* **13,** 365 (1969).
(14) See, e.g., T. A. Halgren, D. A. Kleier, J. H. Hall, Jr., L. D. Brown, and W. N. Lipscomb, *J. Am. Chem. Soc.,* **100,** 6595 (1978); M. J. S. Dewar and G. P. Ford, *ibid.,* **101,** 5558 (1979); J. A. Pople in "Energy, Structure, and Reactivity", D. W. Smith and W. B. McRae, Eds., Wiley, New York, 1973, p 51.
(15) The extended Hückel (EH) method is described by R. Hoffmann and W. N. Lipscomb, *J. Chem. Phys.,* **36,** 2179, 3489 (1962); **37,** 2872 (1962); R. Hoffmann, *ibid.,* **39,** 1397 (1963). The program used is the one reported by D. B. Boyd and W. N. Lipscomb, *J. Theor. Biol.,* **25,** 403 (1969). EH parameters are taken from the 1963 paper, except that $K = 2$ is used as described in the latter paper.
(16) The complete neglect of differential overlap (CNDO/2) method is described by J. A. Pople and D. L. Beveridge, "Approximate Molecular Orbital Theory", McGraw-Hill, New York, 1970. CNDO/2 calculations were done with CNINDO by P. A. Dobosh and C. J. Finder, *QCPE,* **10,** 223 (1972).
(17) The modified intermediate neglect of differential overlap (MINDO/3) method is described by R. C. Bingham, M. J. S. Dewar, and D. H. Lo, *J. Am. Chem. Soc.,* **97,** 1285, 1294, 1302, 1307 (1975); M. J. S. Dewar, D. H. Lo, and C. A. Ramsden, *ibid.,* **97,** 1311 (1975); M. J. S. Dewar, R. C. Haddon, W. K. Li, W. Thiel, and P. K. Weiner, *ibid.,* **97,** 4540 (1975); M. J. S. Dewar, *Chem. Br.,* 11, 97 (1975). Also of interest are the papers by G. Frenking, H. Goetz, and F. Marschner, *J. Am. Chem. Soc.,* **100,** 5295 (1978); T. J. Zielinski, D. L. Breen, and R. Rein, *ibid.,* **100,** 6266 (1978); G. Klopman, P. Andreozzi, A. J. Hopfinger, O. Kikuchi, and M. J. S. Dewar, *ibid.,* **100,** 6267 (1978). The MINDO/3 program used was the one mentioned by F. S. Richardson, C.-Y. Yeh, T. C. Troxell, and D. B. Boyd, *Tetrahedron,* **33,** 711 (1977).
(18) All the ab initio calculations were executed with program PHANTOM by D. Goutier, R. Macauley, and A. J. Duke, *QCPE,* **10,** 241 (1974). Symmetry was used to reduce computation times. A matrix averaging coefficient of 0.25 was employed to stop oscillations in the SCF part of the calculations.
(19) W. J. Hehre, R. F. Stewart, and J. A. Pople, *J. Chem. Phys.,* **51,** 2657 (1969); W. J. Hehre, R. Ditchfield, R. F. Stewart, and J. A. Pople, *ibid.,* **52,** 2769 (1970); J. A. Pople, *Acc. Chem. Res.,* **3,** 217 (1970); L. Radom and J. A. Pople, *J. Am. Chem. Soc.,* **92,** 4876 (1970).
(20) L. C. Snyder and H. Basch, "Molecular Wave Functions and Properties: Tabulated From SCF Calculations in a Gaussian Basis Set", Wiley, New York, 1972.
(21) W. J. Hehre, R. Ditchfield and J. A. Pople, *J. Chem. Phys.,* **56,** 2257 (1972);

W. J. Hehre, *Acc. Chem. Res.*, **9**, 399 (1976); J. A. Pople in "Modern Theoretical Chemistry", Vol. 4, H. F. Schaefer, Ed., Plenum Press, New York, 1977, p 1.
(22) M. Elder, *Int. J. Quantum Chem.*, **7**, 75 (1973).
(23) H. Nakatsuji, *J. Am. Chem. Soc.*, **96**, 30 (1974); G. Herzberg, "Molecular Spectra and Molecular Structure. III. Electronic Spectra and Electronic Structure of Polyatomic Molecules", Van Nostrand, Princeton, N.J., 1967, p 514.
(24) These CNDO/2 calculations were kindly carried out for us by H. H. Jaffé (University of Cincinnati) using his new geometry optimization algorithm.
(25) Some of the advantages and disadvantages of the various techniques for plotting electron-density maps have been reviewed recently by I. Absar and J. R. Van Wazer, *Angew. Chem., Int. Ed. Engl.*, **17**, 80 (1978). It is apparent that certain aesthetic advantages derive from using three-dimensional perspectives of electron-density contours, and that the traditional two-dimensional plotting procedure (such as in Figure 4) remains the only one that clearly and unambiguously shows the exact locations of the nuclei with respect to the contours and at the same time shows more than one contour.
(26) D. B. Boyd, *J. Am. Chem. Soc.*, **94**, 64 (1972); *J. Phys. Chem.*, **78**, 1554, 2604 (1974).
(27) For leading references, see S. Fliszar, *Can. J. Chem.*, **54**, 2839 (1976).
(28) M. J. S. Dewar, R. C. Haddon, A. Komornicki, and H. Rzepa, *J. Am. Chem. Soc.*, **99**, 377 (1977).
(29) K. Hiraoka and P. Kebarle, *Can. J. Chem.*, **53**, 970 (1975); *J. Chem. Phys.*, **63**, 394 (1975); *J. Am. Chem. Soc.*, **98**, 6119 (1976).
(30) L. Radom, D. Poppinger, and R. C. Haddon in "Carbonium Ions", Vol. V, G. A. Olah and P. v. R. Schleyer, Eds., Wiley-Interscience, New York, 1976, p 2329, and references cited therein.
(31) The dispersal of positive charge over the peripheral atoms would be analogous to the dispersal of negative charge studied by R. B. Hermann, *J. Am. Chem. Soc.*, **91**, 3152 (1969); **92**, 5298 (1970).
(32) B. Zurawski, R. Ahlrichs, and W. Kutzelnigg, *Chem. Phys. Lett.*, **21**, 309 (1973).
(33) H. Lischka and H.-J. Köhler, *J. Am. Chem. Soc.*, **100**, 5297 (1978).
(34) For a few other examples, see, for instance, H. Kollmar, H. O. Smith, and P. v. R. Schleyer, *J. Am. Chem. Soc.*, **95**, 5834 (1973); M. J. S. Dewar and R. C. Haddon, *ibid.*, **95**, 5836 (1973); W. J. Hehre and P. v. R. Schleyer, *ibid.*, **95**, 5837 (1973); A. Streitwieser, Jr., and S. Alexandratos, *ibid.*, **100**, 1979 (1978); D. A. Kruse, R. J. Day, W. L. Jorgensen, and R. G. Cooks, *Int. J. Mass Spectrom. Ion Phys.*, **27**, 227 (1978); G. Wenke and D. Lenoir, *Tetrahedron*, **35**, 489 (1979). See also citations by P. P. S. Saluja and P. Kebarle, *J. Am. Chem. Soc.*, **101**, 1084 (1979).

Organized Monolayers by Adsorption. 1. Formation and Structure of Oleophobic Mixed Monolayers on Solid Surfaces

Jacob Sagiv[1]

Contribution from the Max-Planck-Institut für biophysikalische Chemie (Karl-Friedrich-Bonhoeffer-Institut), Abteilung Molekularer Systemaufbau, D-3400 Göttingen, West Germany. *Received May 22, 1978*

Abstract: The possibility of producing oleophobic monolayers containing more than one component (mixed monolayers) is investigated. It is shown that homogeneous mixed monolayers containing components which are very different in their properties and molecular shape may be easily formed on various solid polar substrates by adsorption from organic solutions. Irreversible adsorption may also be achieved through covalent bonding of active silane molecules to the surface of the substrate. Details regarding the structure and the formation of mixed monolayers are revealed by means of spectroscopic methods using surface-active dyes as monolayer components. By studying the time dependence of formation it is shown that interactions involving both the molecules in the adsorbed state and those in solution lead to large fluctuations in the composition of mixed monolayers containing only reversibly adsorbed components, while irreversible adsorption tends to stabilize certain final compositions which are monotonically approached. It is concluded that adsorption on well-defined solid surfaces might be developed into a suitable method for producing monomolecular films with a controllable molecular organization.

I. Introduction

Much of the interest in organic monolayers stems from their relationship to biological membranes. However, their potential use as building elements of artificial systems with completely new properties is by no means less attractive. Kuhn and coworkers have demonstrated that planned structures showing order-dependent properties may be assembled by successive deposition of compressed monolayers formed at the water–air interface[2] (Langmuir–Blodgett monolayers[3]). Although very attractive as a means for handling molecular entities, this technique suffers from certain inherent limitations that will prevent its extension to more sophisticated systems or to large-scale applications. Development of other molecular assembling methods is therefore necessary.

Adsorption of amphipathic molecules on polar solid surfaces has been known to lead under certain conditions to formation of closely packed monomolecular films which are not wetted by organic oils (oleophobic).[4] The existing experimental evidence[5-8] points to a great similarity between the structure of such adsorbed monolayers and of Langmuir–Blodgett monolayers deposited on solid supports from the water–air interface. We have found that oleophobic monolayers containing more than one component (mixed monolayers) can also be produced by adsorption from organic solutions. The incorporation of dyes as components in such mixed monolayers renders layers subject to study by spectroscopic means. A further new development is the production of mixed monolayers containing both chemisorbed and physically adsorbed components.

The purpose of the present and the next two papers in this series is to report our first results in using adsorption on solid surfaces as a method for the production of monolayers with controllable in-plane molecular organization.

II. Adsorption of Mixed Monolayers. Wettability Observations and Desorption Properties

Three main types of mixed adsorbed monolayers were investigated: long-chain saturated fatty acids + long-chain substituted cyanine dyes,[2] *n*-octadecyltrichlorosilane (OTS–$C_{18}H_{37}SiCl_3$) + long-chain substituted cyanine dyes, and fatty acids + OTS. Mixed monolayers containing some other components, as liquid crystals, will be described in part 3. Solutions containing the active components were prepared by dilution of more concentrated stock solutions of fatty acids and dyes in chloroform and of OTS in tetrachloromethane. All solutions were adjusted to a final identical solvent composition of 8% $CHCl_3$ + 12% CCl_4 + 80% *n*-hexadecane (by volume),

0002-7863/80/1502-0092$01.00/0